



The Afflux Calculation Under Effect of Different Number of Vents Experimentally and Using HEC-RAS

Received 4 July 2022; Revised 19 December 2022; Accepted 19 December 2022

Nassar M. A¹

Keywords

Bridges, contraction ratio,
afflux, piers, HEC-RAS

Abstract

The effect of vents' number in bridges for the same contraction ratio was not taken into consideration in many calculation formulas of afflux. The present paper investigates the influence of vents' number on the calculation of the afflux through bridge for the same contraction ratio. The paper experimentally and numerically modeled the water surface profile through the bridge vents to calculate the afflux. The experimental measurements include two stages, the first stage includes the use of a single pier model with a length of 14.7 cm and a width of 2.3 cm. The second stage includes the presence of two piers of 14.7 cm length and 1.15 cm width for each one. The numerical modeling was done using one-dimensional River Analysis System (HEC-RAS). The results showed that the afflux ratio increased as Froude number increased. The increasing of vents' number for the same contraction ratio increases the afflux. The case of contraction ratio = 0.623 gives the higher values of the afflux ratio comparing other contraction ratios. The numerical modeling is promising compared the experimental measurements.

1. Introduction

Afflux as defined in definitions website is the upstream water rise of a bridge [6]. One of the important formulas used to calculate afflux is Vector formula (1980) [Eq. 1] as presented in Parry & Jones [15].

$$AF = \frac{v^2}{2g} \left(\frac{b^2}{c^2 N z^2} - 1 \right) \quad (1)$$

In which: AF is the afflux, b is the channel width upstream the bridge, g is the gravitational acceleration, " c " a constant, v is the flow velocity downstream the bridge and N is the number of the bridge vents, see figure (1).

¹ Water Engineering and Water Structures Department, Faculty of Engineering, Zagazig University, Egypt.
nasserzagazig@yahoo.com

Many researchers investigated the contractions in open channels among of them [10], [11], [18], [19] and [21]. Fahmy and Nassar [2] investigated flow and scour characteristics under effect of contraction upstream abutments.

Application of simulation software is the most famous trend in the last decade, especially in the field of hydraulics. Nassar et al, [9] applied support vector machines as an artificial intelligence tool to predict the scour depth downstream gates. Negm, et al. [12] investigated the ability of ANN model to forecast suspended sediment. Nassar, [8] developed a one-dimensional mathematical model to simulate water stage in open channels. Habib & Nassar [5] simulated the erosion and deposition through a 180° open canal bend by Nays2DH model in iRIC software. Shimizu, et al. [17] defined outcomes from computational modelling of flow and sediment for many applications using iRIC software. None's, et al. [13] presented a numerical modelling of a reach of the Po River using iRIC software. The results presented hopeful abilities of the model. Rai, et al. [16] simulated flood scenarios using iRIC & SWAT and SWMM models.

Mehta & Yadav [7] applied HEC-RAS to simulate the scour around Sardar bridge on Tapi river. Ghaderi, et al. [4] investigated scour at piers of Simineh bridge in Iran empirically and using HEC-RAS model. Noor, et al. [14] applied HEC-RAS to model the scour around piers. Subedi, et al. [20] hydraulically simulate the flow around bridges using HEC-RAS. It was indicated that, the water surface rises as the flow area decreased.

The review showed that vents' number for the same contraction ratio was not taken into consideration through the calculation process of afflux. The influence of the vents' number on the calculation of the afflux was investigated in the present paper. The paper experimentally and numerically modelled the water surface profile through the bridge vents. The numerical modelling was done using River Analysis System (HEC-RAS).

2. Methods

2.1. Dimensional analysis

The afflux through bridges is proposed to be defined using the dimensionless equation (2). The experimental models describe the phenomenon is presented in the sketch shown in figure (1).

$$\Delta AF = \Phi(FR, Cont, \frac{V_5^2}{2g}, N) \quad (2)$$

In which, ΔAF is the afflux ratio = $\frac{d_1 - d_5}{d_1}$, d_1 and d_5 are flow depths upstream and downstream the pier, see figure (1), FR is Froude number at the normal depth upstream the bridge, $Cont$ is the contraction ratio due to the presence of the pier = $\frac{Nz}{b}$, N is the number of the bridge vents, z is the vent width, b is the channel width upstream the bridge, V_5 is the average channel flow velocity downstream the bridge, and g is the gravitational acceleration.

2.2. Experimental works

The laboratory experiments were carried out in the fluid mechanics laboratory, faculty of engineering, Umm Al-Qura university in Al-Qunfudhah. The laboratory channel was 7.7 cm width, 15 cm depth, and the total length is 110 cm. A moving ruler was used to measure the flow at different depths. The flow discharge passing through the channel was measured using a digital flowmeter. The wooden models representing the bridge piers were installed at the bottom of the channel using adhesives material, see figure (1).

The collected laboratory measurements include two stages, see table (1): The first stage includes the use of a single pier model with a length of 14.7 cm and a pier width of 2.3 cm, see figures (1b and 1c). The second stage of laboratory measurements includes the presence of two piers of 14.7 cm length and 1.15 cm width for each one.

Table. 1: The characteristics of the laboratory measurements

	$Cont = \frac{Nz}{b}$	Number of vents	Number of Collected runs	The vent' width (cm)	The piers' width (cm)
Stage I	0.701	2	6	2.7	2.3
Stage II	0.701	3	6	1.8	1.15

2.3. HEC-RAS model

The public domain software River Analysis System (HEC-RAS) performs steady and unsteady 1D & 2D hydraulics calculations (Brunner & CEIWR-HEC) [3]. It can perform the calculations for the water surface profiles in the case of steady flow. In addition, it performs the computations of sediment transport, and water quality. The building of 1D HEC-RAS Model for the steady flow in open channels to simulate the water surface profile under different contraction ratios includes 4-steps. These steps can be listed as following:

- Prepare the geometric data,
- Input the steady flow data,
- Performing the steady flow simulation and
- View the results

The geometric data are prepared in a separate window as shown in figure (2a). It clears that, the studied reach includes 4- sections. Sections 3 and 4 include the bridge vents, while the other section are the rectangular of width = 0.77m. All sections data are edited in HEC-RAS model as seen in figure (2b).

The bed slope was taken = 0.001 or 0.0013. The total numerical tests are 69 runs. All details of the numerical tests are shown in table (2). The steady flow data includes the flow discharge and the boundary conditions. The flow discharge was varied between (0.003 to 0.008) m³/sec. The boundary condition was taken as normal depth with slope of 0.001:0.0013, see figure (3a). The next step is running computations, see figure (3b). The results are displaying as shown in figure (4). It includes the water surface profile and the flow velocity see figures (4a and 4b), respectively.

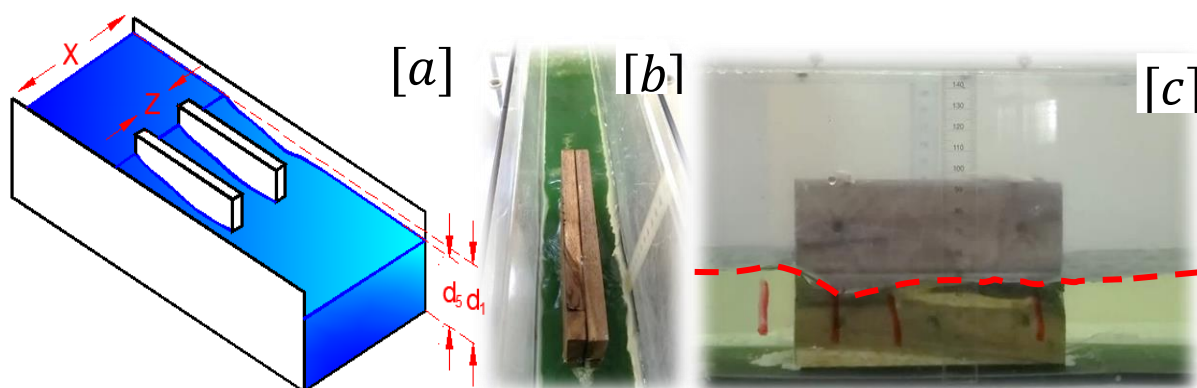


Fig. 1: [a] isometric of three vents bridge [b] a plan photo of the experimental model [c] an elevation photo of the experimental model

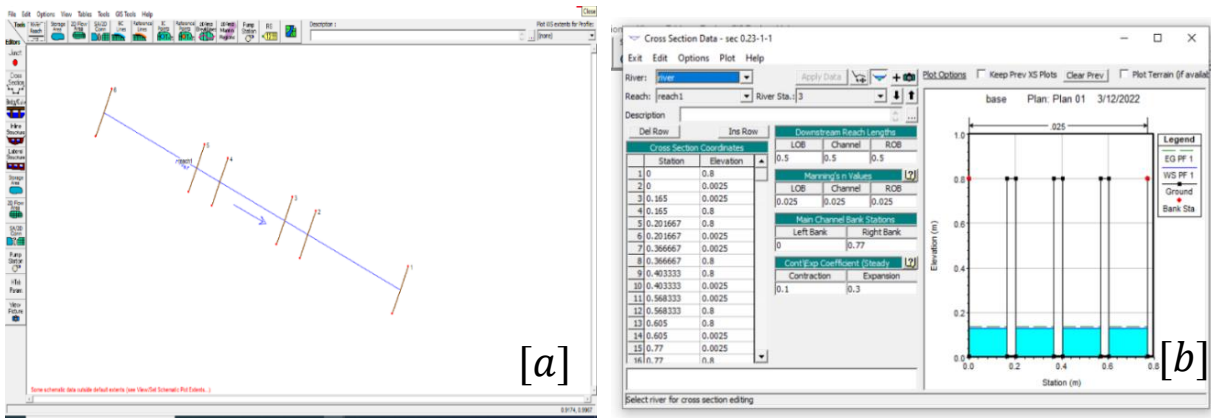


Fig. 2: [a] the window of the generated river reaches in HEC-RAS model [b] the window of the generated cross sections in HEC-RAS model

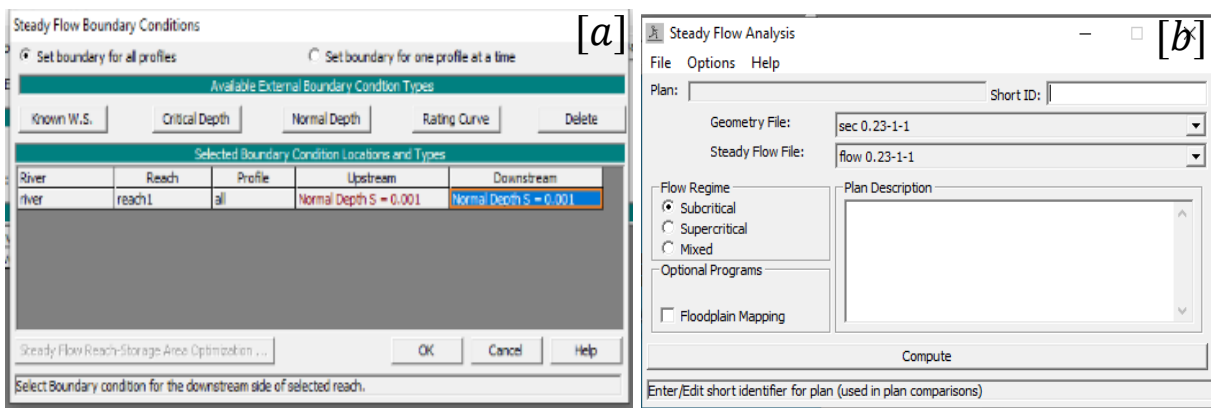


Fig. 3: [a] the window of the input flow data to HEC-RAS model [b] the window of the computation process

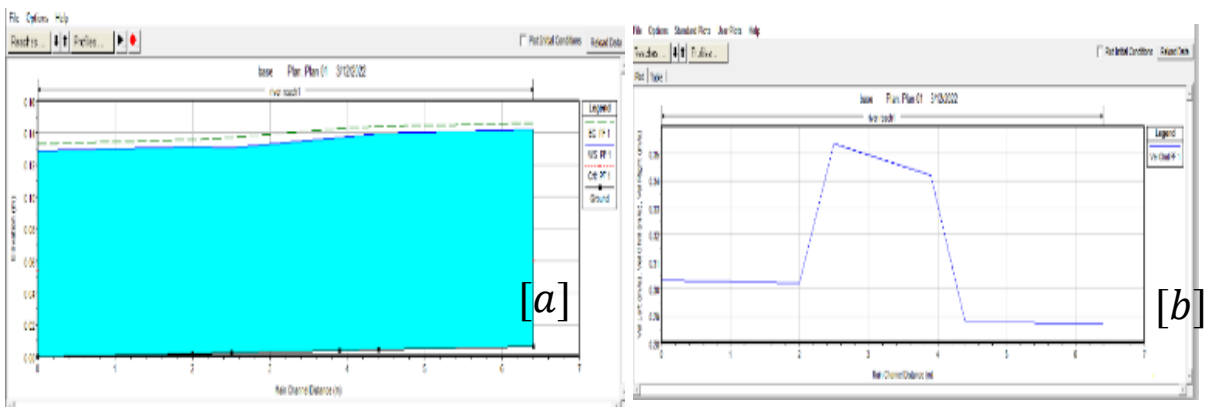
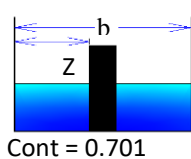
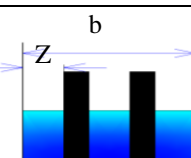
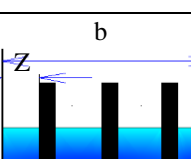


Fig. 4: outputs samples of HEC-RAS [a] water surface profile [b] flow velocity

Table. 2: The generated geometric data in HEC-RAS models

Stage	case	Cont	Number of vents	Number of Collected runs	The piers' width (m)	sketch
I	1	0.623	2	6	0.029	 Cont = 0.701
	2	0.701		7	0.023	
	3	0.779		6	0.017	
	4	0.857		6	0.011	
II	1	0.623	3	6	0.0145	
	2	0.701		7	0.0115	
	3	0.779		6	0.0085	
	4	0.857		5	0.0055	
III	1	0.623	4	5	0.0096	
	2	0.701		5	0.0076	
	3	0.779		5	0.0056	
	4	0.857		5	0.0036	

3. Results

3.1. Experimental outputs

The results of laboratory measurements were presented as shown in figure (5). Figure (5a) presents the relationship between the afflux ratio ΔAF and Froude number FR for the different experimental stages. It can be seen that, ΔAF increased as FR increased for the experimental measurements. It is obvious that, stage II ($N=3$ & $Cont = 0.701$) gives the higher values of the afflux ratio ΔAF comparing stage I, see figure (5a). It can be said that the increasing of the vents' number through the channel for the contraction ratio = 0.701 increasing the afflux ratio ΔAF .

Figure (5b) presents a relation between the afflux ratio ΔAF , versus Froude number FR for the differential experimental stages and that computed by Vector formula (1980). It clears that, calculations of the afflux ratio ΔAF for the experimental stages are not matched with that calculated by Vector formula (1980). The experimental results for the same contraction ratio scattered around the trend curve of Vector formula (1980). It can be said that the vents' number for the same contraction ratio is obviously affect the correlation between experimental measures and Vector formula (1980).

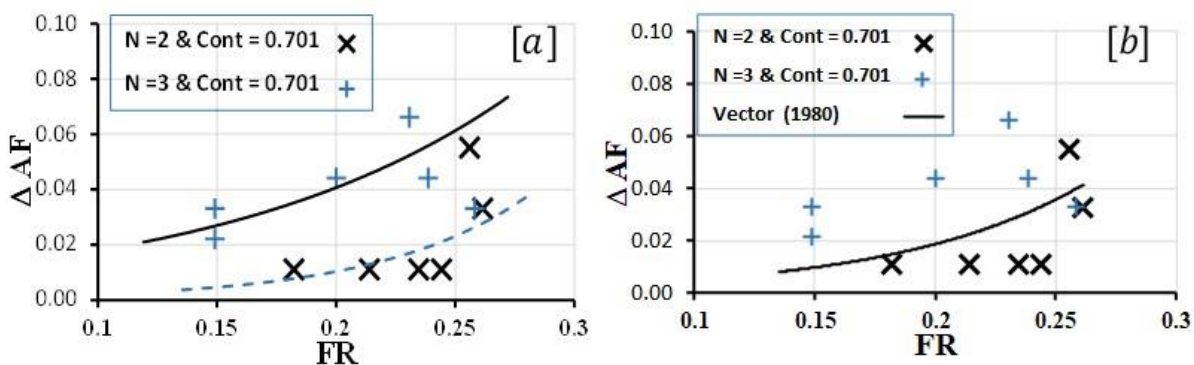


Fig. 5: [a] the relationship between ΔAF and FR for the experimental stages [b] the relationship between ΔAF and FR for the experimental stages and Vector formula (1980)

3.2. 1D HEC-RAS outputs

Figures 6, 7 and 8 show samples of the water surface profiles calculated by HEC-RAS model for different Froude number FR and the same contraction ratio. The calculated water surface profiles by HEC-RAS were used to calculate the values of afflux ΔAF .

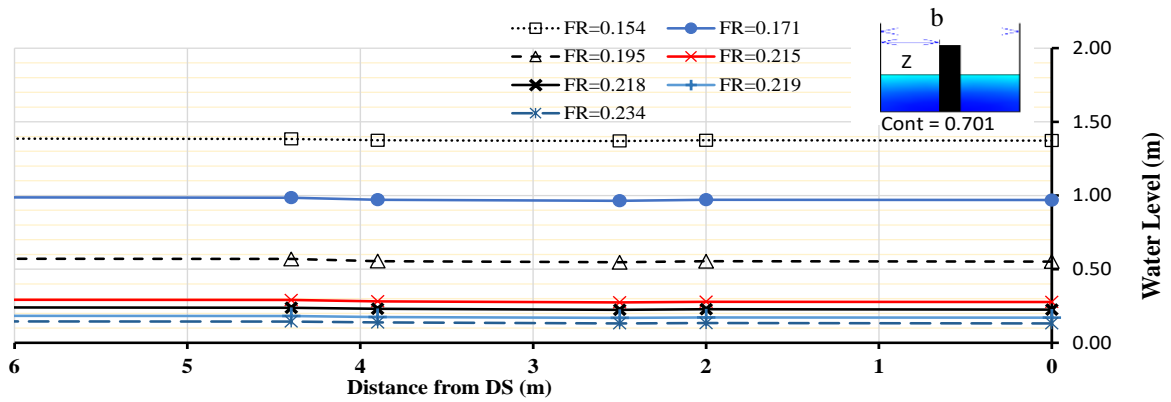


Fig. 6: samples of the water surface profiles of HEC-RAS for $N = 2$ & $Cont. = 0.701$

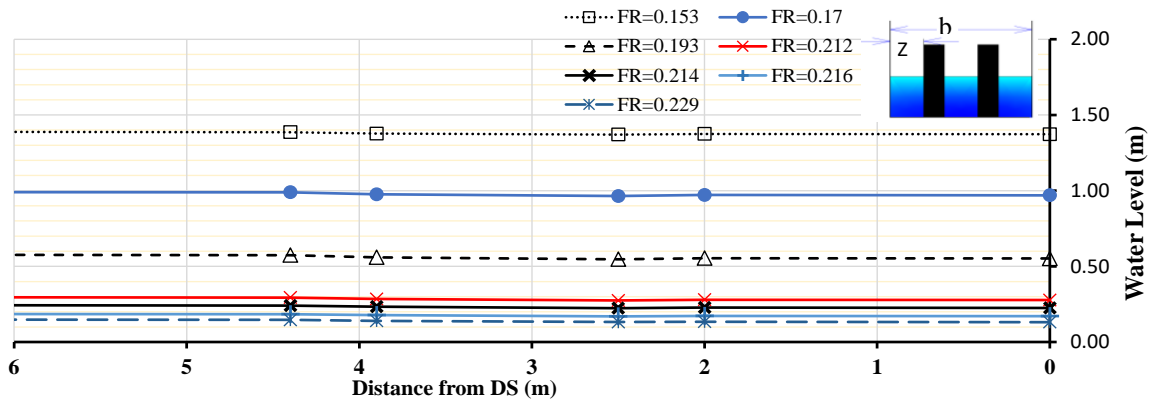


Fig. 7: samples of the water surface profiles of HEC-RAS for $N = 3$ & $Cont. = 0.701$

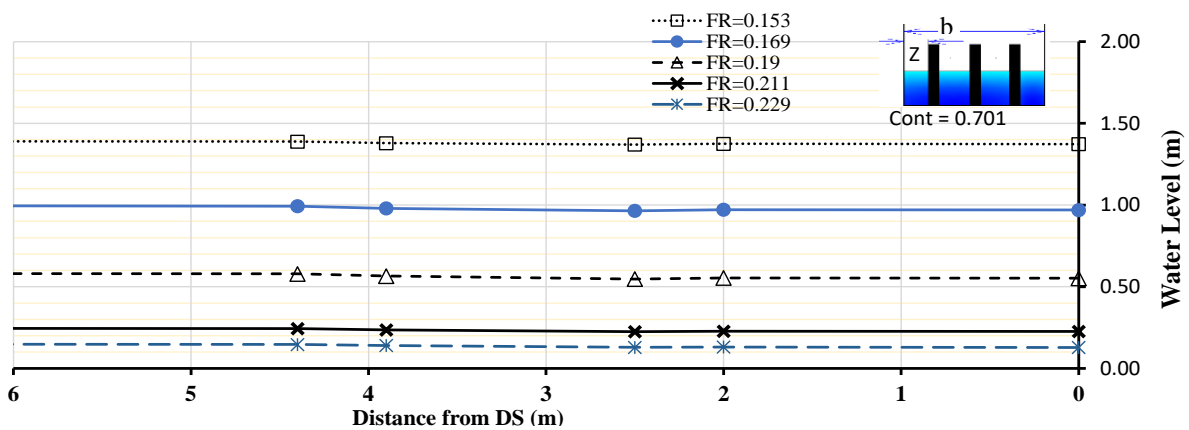


Fig. 8: samples of the water surface profiles of HEC-RAS for $N = 4$ & $Cont = 0.701$

3.3. Statistical Analysis

The multiple linear regression is applied to generate the equation used to calculate the afflux ΔAF . The equation is generated depending on the theoretical formula shown in Eq. (2). The generated equation is presented as Eq. (3). The collected values calculated by HEC-RAS outputs were divided

into two groups including training and validation. The percentage of the training values = 82% used to generate Eq. (3). The validation data of 18% were used to evaluate the equation for data out of the training community. The limitation of the generated equation (3) is tabulated in table (3). It clearly shown that Eq. (3) is powerful.

$$\Delta AF = 0.00453 + 0.50737 \times FR - 0.10603 \times Cont - 1.04103 \times \frac{V_5^2}{2g} + 0.00647 \times N \quad (3)$$

Table. 3: Limitation of Eq. (3)

Item	FR	$Cont$	$\frac{V_5^2}{2g}$	N
Maximum	0.2524	0.8571	0.0164	4
Minimum	0.1520	0.6233	0.0044	2

Table. 4: Statistics of Eq. (3)

Item	Training	Validation
Multiple R	0.9491	0.9650
R Square	0.9008	0.9312
RMSE	0.0060	0.0199

4. Discussion

The outputs of HEC-RAS Model are compared to the experimental measurements for two cases: the first one includes ($N = 2$ & $Cont = 0.701$), see figure (9a). The second one includes the case of ($N = 3$ & $Cont = 0.701$), see figure (9b). It clears that, the calculated values of afflux ratio ΔAF using HEC-RAS Model for the case of ($N = 2$ & $Cont = 0.701$) are close to the experimental values for $FR < 0.2$, see figure (9a). The calculated values of afflux ratio ΔAF using HEC – RAS Model for the case of ($N = 3$ & $Cont = 0.701$) are very close the experimental values. It can be said that there is a matching between the outputs of HEC-RAS Model and the collected measurements for $FR < 0.2$. A general speaking, HEC-RAS Model, gives an acceptable output comparing in the lab measurements see figure (9).

The investigated relations which were calculated using HEC-RAS outputs are the relationships between ΔAF and FR . It was presented in figure (10a, 10b and 10c) for the different values of contraction ratios, $N = 2$, $N = 3$ and $N = 4$, respectively. The figures show that, ΔAF increased as FR increased for the numerical outputs of HEC-RAS model. In addition, the decreasing of the contraction ratio through the channel for the same FR increasing the ratio of afflux ΔAF . It is obvious that, the case of $Cont = 0.623$ gives the higher values of the afflux ratio ΔAF comparing other cases, see figure (10). Figures (11) display the relationships between the ratio of afflux ΔAF versus Froude number FR calculated by HEC-RAS outputs for the different number of vents and constant contraction ratios. It clears that, the increasing of the vents number through the channel for the same contraction ratio increasing the ratio of afflux ΔAF . It is obvious that, the case of $N = 4$ gives the higher values of the afflux ratio ΔAF comparing other cases, see figure (11). Figure (12) compares between calculated values by Eq. (3) and that using HEC-RAS. There is an acceptable agreement between Eq. (3) and detected ones using HEC-RAS, see fig. (12).

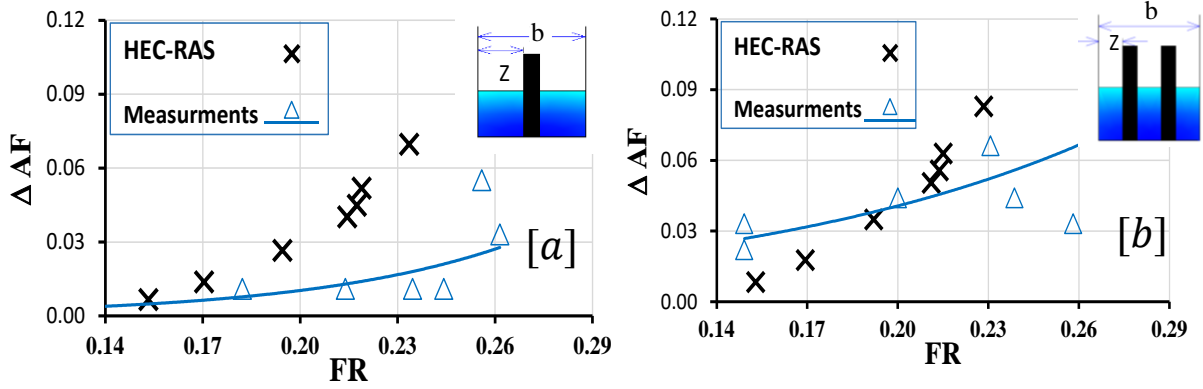


Fig. 9: the relationship between ΔAF and FR for the experimental measurements and HEC-RAS outputs [a] ($N=2$ & $Cont = 0.701$) [b] ($N = 3$ & $Cont = 0.701$)

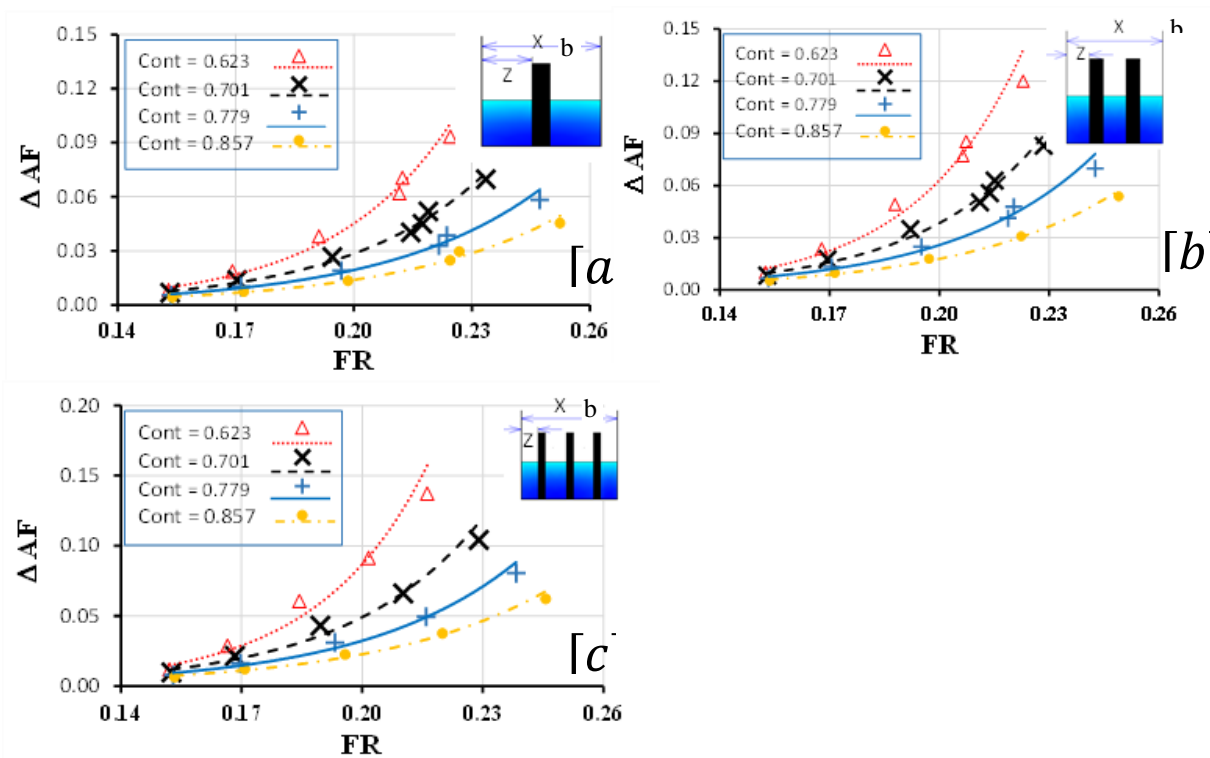


Fig. 10: the relationships between the ratio of afflux, ΔAF versus Froude number FR calculated by HEC-RAS for the different contraction ratios [a] $N=2$ [b] $N=3$ [c] $N=4$

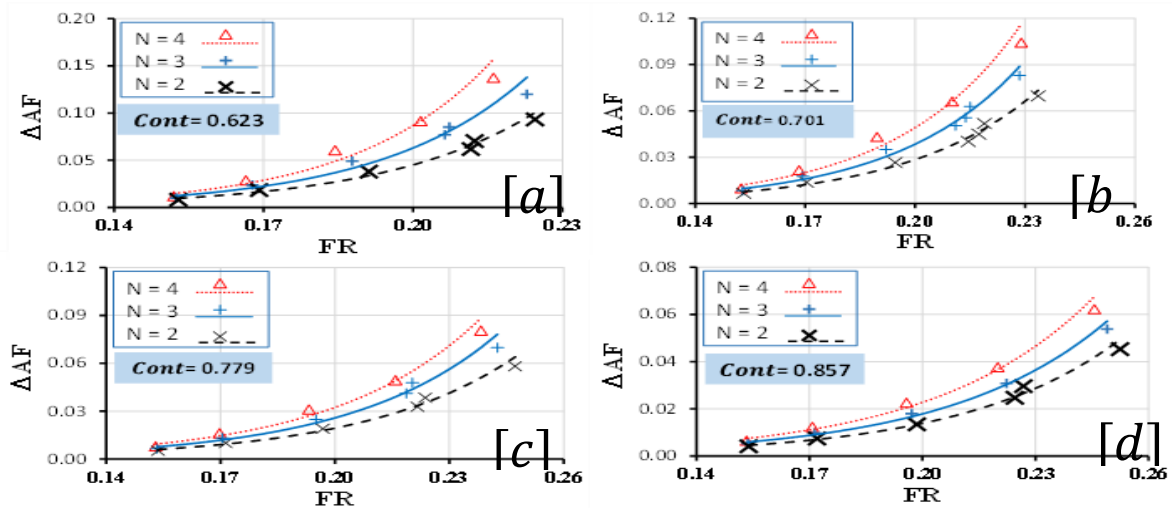


Fig. 11: the relationships between ΔAF versus FR for HEC-RAS outputs in case of the different vents number and constant contraction ratios [a] Cont. =0.623 [b] Cont. =0.701 [c] Cont. =0.779 [d] Cont. =0.857

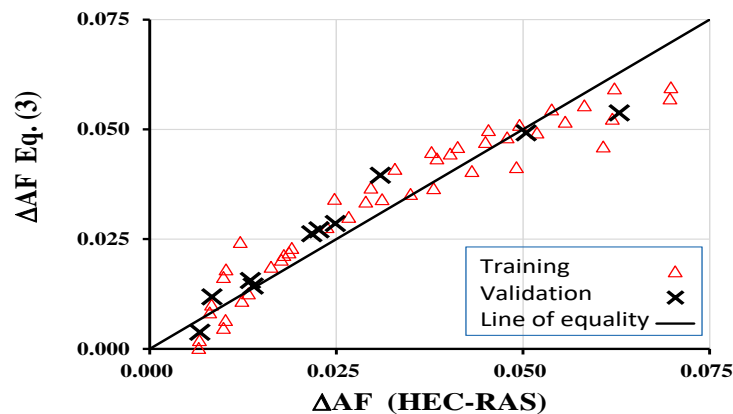


Fig. 12: Eq. (3) against HEC-RAS values

5. Conclusions

The paper examines the influence of number of vents on the calculation of the afflux through bridge. The following points can be concluded.

- The afflux ratio ΔAF increased as FR increased.
- The experimental measuring shows that the increasing of the vents' number through the channel for the contraction ratio = 0.701 increasing the afflux ratio ΔAF .
- The experimental measuring shows that the vents' number for the same contraction ratio is obviously affect the correlation between experimental measures and Vector formula (1980).
- The outputs of HEC-RAS model show that the decreasing of the contraction ratio for the same FR increasing the afflux ratio ΔAF , that matches the results presented by Subedi, et al. (2019).
- The case of contraction ratio = 0.623 gives the higher values of the afflux ratio ΔAF comparing other cases.
- The case of $N = 4$ gives the higher values of the afflux ratio ΔAF comparing other cases.
- The multiple linear regression is applied to generate a powerful equation to calculate the afflux ΔAF .

References

- [1]. Dawson, J. H. (1943). The effect of lateral contractions on super-critical flow in open channels.
- [2]. Fahmy M.R., and Nassar M. A., (2017), Contraction effect upstream abutments on velocity and scour: experimental and theoretical study using IRiC software, *Journal of Engineering Sciences Assiut University Faculty of Engineering* Vol. 45 No. 1 January 2017. doi: <https://doi.org/10.21608/jesaun.2017.116082>
- [3]. Gary W. Brunner & CEIWR-HEC, (2021), “HEC-RAS, River Analysis System User's Manual Version 6.0”, US Army Corps of Engineers Institute for Water Resources Hydrologic Engineering Center.
- [4]. Ghaderi, A., Daneshfaraz, R., & Dasineh, M. (2019). Evaluation and prediction of the scour depth of bridge foundations with HEC-RAS numerical model and empirical equations, *Engineering Journal* 23 (6), doi: <https://doi.org/10.4186/ej.2019.23.6.279>
- [5]. Habib, A. A., & Nassar, M. A. (2019). Modelling of Deposition and Erosion Processes Along a 180° Open Canal Bend by Nays2dh in iRIC. *Engineering Heritage Journal (GWK)*, 3(2), 01-05. doi: <https://doi.org/10.26480/gwk.02.2019.01.05>
- [6]. <https://www.definitions.net/definition/afflux>
- [7]. Mehta, D. J., & Yadav, S. M. (2020). Analysis of scour depth in the case of parallel bridges using HEC-RAS. *Water Supply*, 20(8), 3419-3432. doi: <https://doi.org/10.2166/ws.2020.255>
- [8]. Nassar, M. A. (2010). One-dimensional hydrodynamic model simulating water stage in open channels (ws-1). *International Journal of Modeling, Simulation, and Scientific Computing*, 1(02), 303-316. doi: <https://doi.org/10.1142/s1793962310000110>
- [9]. Nassar, M. A., Ibrahim, A. A., & Negm, A. M. (2009). Modeling of Local Scour Down Stream of Hydraulic Structures Using Support Vector Machines (SVMS). In *Proc. Of 6th Int. Conf. on Environmental Hydrology*, Cairo, Egypt.
- [10]. Negm, A. M., Elfiky, M. M., Attia, M. I., & Ezzeldin, M. M. (2003a), Energy loss due to sudden contraction through transition length in sloped open channels. *Proc. of 7th Alazhar Engineering Int. Conf. April 7-10, Faculty of Engineering, Alazhar University, Naser City, Cairo, Egypt, 2003.*
- [11]. Negm, A. M., Elfiky, M. M., Attia, M. I., & Ezzeldin, M. M. (2003b), protection length downstream of sudden transition for incoming subcritical flow, *1st International Conference of Civil Engineering Science, ICCES1, Vol. 1.*
- [12]. Negm, A. M., Elfiky, M. M., Owais, T. M., & Nassar, M. H. (2003). Prediction of suspended sediment concentration in river flow using artificial neural networks. In *Proceedings of 6th International Conference On River Engineering*, Ahvaz, Iran. doi:
- [13]. Nones, M., Pugliese, A., Domeneghetti, A., & Guerrero, M. (2018). Po River morphodynamics modelled with the open-source code iRIC. In *Free Surface Flows and Transport Processes* (pp. 335-346). Springer, Cham. doi: https://doi.org/10.1007/978-3-319-70914-7_22
- [14]. Noor, M., Arshad, H., Khan, M., Khan, M. A., Aslam, M. S., & Ahmad, A. (2020). Experimental and HEC-RAS Modelling of Bridge Pier Scouring. *Journal of Advanced Research in Fluid Mechanics and Thermal Sciences*, 74(1), 119-132. doi: <https://doi.org/10.37934/arfmts.74.1.119132>
- [15]. Parry, J. D., & Jones, T. E. (1992). *A design manual for small bridges*. TRL Transport Research Laboratory.
- [16]. Rai, P. K., Dhanya, C. T., & Chahar, B. R. (2018). Coupling of 1D models (SWAT and SWMM) with 2D model (iRIC) for mapping inundation in Brahmani and Baitarani river delta. *Natural Hazards*, 92(3), 1821-1840. doi: <https://doi.org/10.1007/s11069-018-3281-4>
- [17]. Shimizu, Y., Nelson, J., Arnez Ferrel, K., Asahi, K., Giri, S., Inoue, T., & Yamaguchi, S. (2020). Advances in computational morphodynamics using the International River Interface Cooperative (iRIC) software. *Earth Surface Processes and Landforms*, 45(1), 11-37. doi: <https://doi.org/10.1002/esp.4653>
- [18]. Skogerboe, G. V., & Hyatt, M. L. (1968). Rating Side Contractions in Open Channels. *Journal of the Irrigation and Drainage Division*, 94(1), 181-183. doi: <https://doi.org/10.1061/jrcea4.0000555>
- [19]. Sturm, T. W. (1985). Simplified design of contractions in supercritical flow. *Journal of Hydraulic Engineering*, 111(5), 871-875. doi: [https://doi.org/10.1061/\(asce\)0733-9429\(1985\)111:5\(871\)](https://doi.org/10.1061/(asce)0733-9429(1985)111:5(871))
- [20]. Subedi, A. S., Sharma, S., Islam, A., & Lamichhane, N. (2019). Quantification of the effect of bridge pier encasement on headwater elevation using HEC-RAS. *Hydrology*, 6(1), 25. doi:

<https://doi.org/10.3390/hydrology6010025>

- [21]. Wu, B., & Molinas, A. (2001). Choked flows through short contractions. *Journal of Hydraulic Engineering*, 127(8), 657-662. doi: [https://doi.org/10.1061/\(asce\)0733-9429\(2001\)127:8\(657\)](https://doi.org/10.1061/(asce)0733-9429(2001)127:8(657)).

حساب ارتفاع ارتداد المياه تحت تأثير فتحات مختلفة خلال الكباري تجريبياً وباستخدام HEC-RAS

الملخص العربي

لا شك ان تأثير عدد فتحات الكباري لنفس نسبة الاختناق لم يؤخذ تأثيره بشكل وافي عند احتساب ارتفاع ارتداد الماء أمام الكباري وقد قام البحث الحالي بتقديم دراسة تجريبية وعددية باستخدام برنامج HEC-RAS على تأثير عدد فتحات الكباري لنفس نسبة الاختناق تشمل القياسات التجريبية مرحلتين، المرحلة الأولى تتضمن استخدام نموذج دعامة واحدة بطول ١٤,٧ سم وعرض ٢,٣ سم. وتشمل المرحلة الثانية وجود دعامتين بطول ١٤,٧ سم وعرض ١,١٥ سم لكل منهما. تم إجراء النمذجة العددية باستخدام برنامج أحادي الابعاد (HEC-RAS) أظهرت النتائج العملية إنه يحدث زيادة في قيمة الارتداد مع زيادة في رقم فرويد كما بينت النتائج أن زيادة عدد الفتحات لنفس نسبة الاختناق يزيد من قيمة الارتداد وخلال حدود الدراسة اتضح ان نسبة الاختناق = ٠,٦٢٣ تعطي اعلي قيمة لنسبة الارتداد مقارنة بالنسب الأخرى. كما بينت الدراسة ان الدراسة الرقمية باستخدام برنامج (HEC-RAS) واعدة مقارنة بالقياسات التجريبية